

Diet-Induced Obesity and Reduced Skin Cancer Susceptibility in Matrix Metalloproteinase 19-Deficient Mice

Alberto M. Pendás,^{1*} Alicia R. Folgueras,¹ Elena Llano,^{1†} John Caterina,²
Françoise Frerard,³ Francisco Rodríguez,¹ Aurora Astudillo,⁴
Agnès Noël,³ Henning Birkedal-Hansen,²
and Carlos López-Otín¹

Departamento de Bioquímica y Biología Molecular, Facultad de Medicina, Instituto Universitario de Oncología, Universidad de Oviedo,¹ and Servicio de Anatomía Patológica, Hospital Central de Asturias,⁴ Oviedo, Spain; MMP Unit, National Institute of Dental and Craniofacial Research, Bethesda, Maryland 20892²; and Laboratory of Tumor and Developmental Biology, Université de Liège, B-4000 Liège, Belgium³

Received 22 March 2004/Accepted 26 March 2004

Matrix metalloproteinase 19 (MMP-19) is a member of the MMP family of endopeptidases that, in contrast to most MMPs, is widely expressed in human tissues under normal quiescent conditions. MMP-19 has been found to be associated with ovulation and angiogenic processes and is deregulated in diverse pathological conditions such as rheumatoid arthritis and cancer. To gain further insights into the in vivo functions of this protease, we have generated mutant mice deficient in *Mmp19*. These mice are viable and fertile and do not display any obvious abnormalities. However, *Mmp19*-null mice develop a diet-induced obesity due to adipocyte hypertrophy and exhibit decreased susceptibility to skin tumors induced by chemical carcinogens. Based on these results, we suggest that this enzyme plays an in vivo role in some of the tissue remodeling events associated with adipogenesis, as well as in pathological processes such as tumor progression.

The matrix metalloproteinases (MMPs) are a group of zinc-dependent endopeptidases that play major roles in the connective tissue remodeling occurring in a variety of physiological conditions such as embryonic growth and development, angiogenesis and wound healing (5, 28, 40). In addition, deregulated production of these enzymes is associated with multiple pathological conditions, including rheumatoid arthritis (19), atherosclerosis (13), and tumor invasion and metastasis (11, 12). The human MMP family is composed of more than 20 different members that can be classified into different subfamilies according to their primary structures, domain organization, cellular localization, and substrate specificity (5, 28).

As part of our studies focused on the structural and functional characterization of this protein family, we have recently cloned a new human MMP that has been designated MMP-19 (32). This protease shows the archetypal domain organization of soluble MMPs, including a signal sequence, a propeptide with the cysteine residue essential for maintaining latency, a catalytic domain with the typical zinc-binding motif, a linker region, and a C-terminal fragment with sequence similarity to hemopexin (32). However, MMP-19 lacks several structural features distinctive of the diverse MMP subfamilies and possesses a unique insertion of glutamic acid residues within the linker region. It also exhibits an unusual latency motif in the propeptide domain, an additional cysteine residue in the catalytic region, and a C-terminal extension lacking sequence

similarity to equivalent regions in other human MMPs (7, 32, 41). MMP-19 is widely distributed in human tissues, which is also a distinctive feature of this MMP, because most family members are not frequently produced by adult cells under normal quiescent conditions. Accordingly, we and others have suggested that this enzyme could play a role in some of the normal matrix remodeling processes that take place in tissues with the ability to produce MMP-19 (27, 32). Biochemical studies have revealed that MMP-19 shows a potent basement membrane-degrading activity and is also capable of degrading two components of cartilage, namely, cartilage oligomeric matrix protein and aggrecan (38, 39). Interestingly, MMP-19 has also been identified as an autoantigen in patients with rheumatoid arthritis (36), and recent studies have suggested a role for this enzyme in angiogenic processes (18). Therefore, according to its unique structural features and tissue distribution, MMP-19 could represent the first member of a new subfamily of MMPs with a critical and novel role in physiological or pathological conditions. To try to uncover the function of this protease, we have generated mutant mice lacking *Mmp19*. These mice are viable and fertile and do not show any overt phenotype. However, after a series of different experimental challenges performed on wild-type and mutant mice, we provide evidence that *Mmp19*-null mice develop a diet-induced obesity and exhibit decreased susceptibility to skin tumors induced by chemical carcinogens. Based on these results, we suggest that this enzyme plays an in vivo role in some of the tissue remodeling events associated with adipogenesis and tumor progression.

MATERIALS AND METHODS

Targeting vector construction. A genomic DNA clone was isolated from a mouse 129-SV/J genomic DNA library (Stratagene, La Jolla, Calif.) by using a murine *Mmp19* cDNA fragment as probe. The genomic organization was deter-

* Corresponding author. Mailing address: Departamento de Bioquímica y Biología Molecular, Facultad de Medicina, Universidad de Oviedo, 33006 Oviedo, Spain. Phone: 34-985-104201. Fax: 34-985-103564. E-mail: amp@correo.uniovi.es.

† Present address: Centro Nacional de Investigaciones Oncológicas, Madrid, Spain.

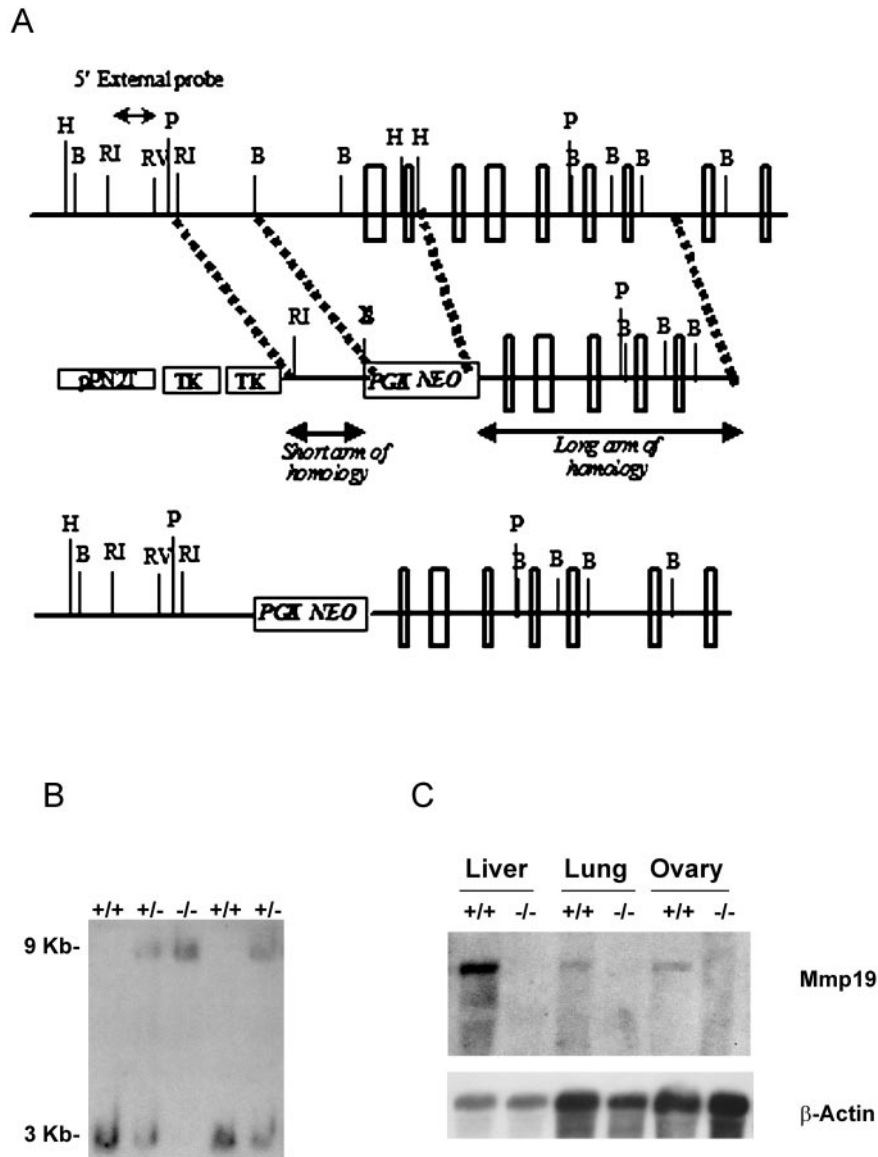


FIG. 1. Targeted disruption of mouse *Mmp19* gene. (A) Restriction maps of the *Mmp19* gene region of interest (top), the targeting construct (center), and the mutant locus after homologous recombination (bottom). B, BamHI; B with superimposed X, destroyed BamHI; H, HindIII; P, PstI; RI, EcoRI; RV, EcoRV. (B) BamHI Southern blot analysis of +/+, +/-, and -/- mice. (C) Detection of *Mmp19* mRNA in the liver, lung, and ovary by Northern blot analysis.

mined by restriction analysis and subsequent subcloning of these fragments into pBluescript or pUC18. The genomic region immediately surrounding the first exon was sequenced and showed characteristic elements of a typical MMP promoter region such as an AP-1 site and a TATA box (31). Plasmid pPN2T-Hgterm (kindly provided by C. Paszty, Lawrence Berkeley National Laboratory, Berkeley, Calif.) containing the *pgk-neo* and two *pgk-tk* (thymidine kinase) selection markers was used to construct the *Mmp19* targeting vector. A 1.6-kb EcoRI-BamHI fragment from the 5'-flanking region was used as the 5'-homologous region, whereas a 6-kb XhoI-NotI fragment containing exons 3 to 8 was used as the 3'-region of homology. The 2.4-kb *neo* cassette was used as a positive marker and replaced a 3-kb fragment containing 1 kb of promoter and exons 1 and 2 of the gene (Fig. 1A). After both fragments were cloned, the BamHI restriction site of the short arm was destroyed by digestion and blunt-ended religation to further generate a BamHI RFLP in the targeted allele.

Generation of *Mmp19*-null mice. The targeting vector was linearized by digestion with NotI, electroporated into HM-1 embryonic stem (ES) cells, and se-

lected for homologous recombination with G418 and ganciclovir. Positive clones were screened by Southern blot after BamHI digestion of genomic DNA and probed with a radiolabeled 5'-external probe (Fig. 1B). A 3-kb fragment was detected from the wild-type allele and a 9-kb fragment from the mutant allele. The targeted ES cell clones were expanded and subsequently injected into blastocysts to generate chimeras. Chimeric males were mated with black female mice and the offspring heterozygous for *Mmp19*^{+/-} were used to generate homozygous null mice. Mice genotypes were determined by Southern blot analysis of tail DNA.

Northern blot analysis. Total RNA from frozen subcutaneous (SC) and gonadal (GON) adipose tissue was isolated by using a commercial kit (RNeasy Mini Kit; Qiagen). A total of 10 μg of denatured RNA was resolved by electrophoresis on 1.2% agarose gels and transferred to Hybond N+ (Amersham Pharmacia Biotech). Blots were hybridized with random primed ³²P-labeled cDNA probes for mouse *Mmp19* (AAF73292), *Pparγ*, *Serbp1*, *leptin*, and *Mrp2*. Probes were obtained by using reverse transcriptase PCR from adipose tissue RNA. The following sets of primers were used for PCR amplification: *Pparγ*

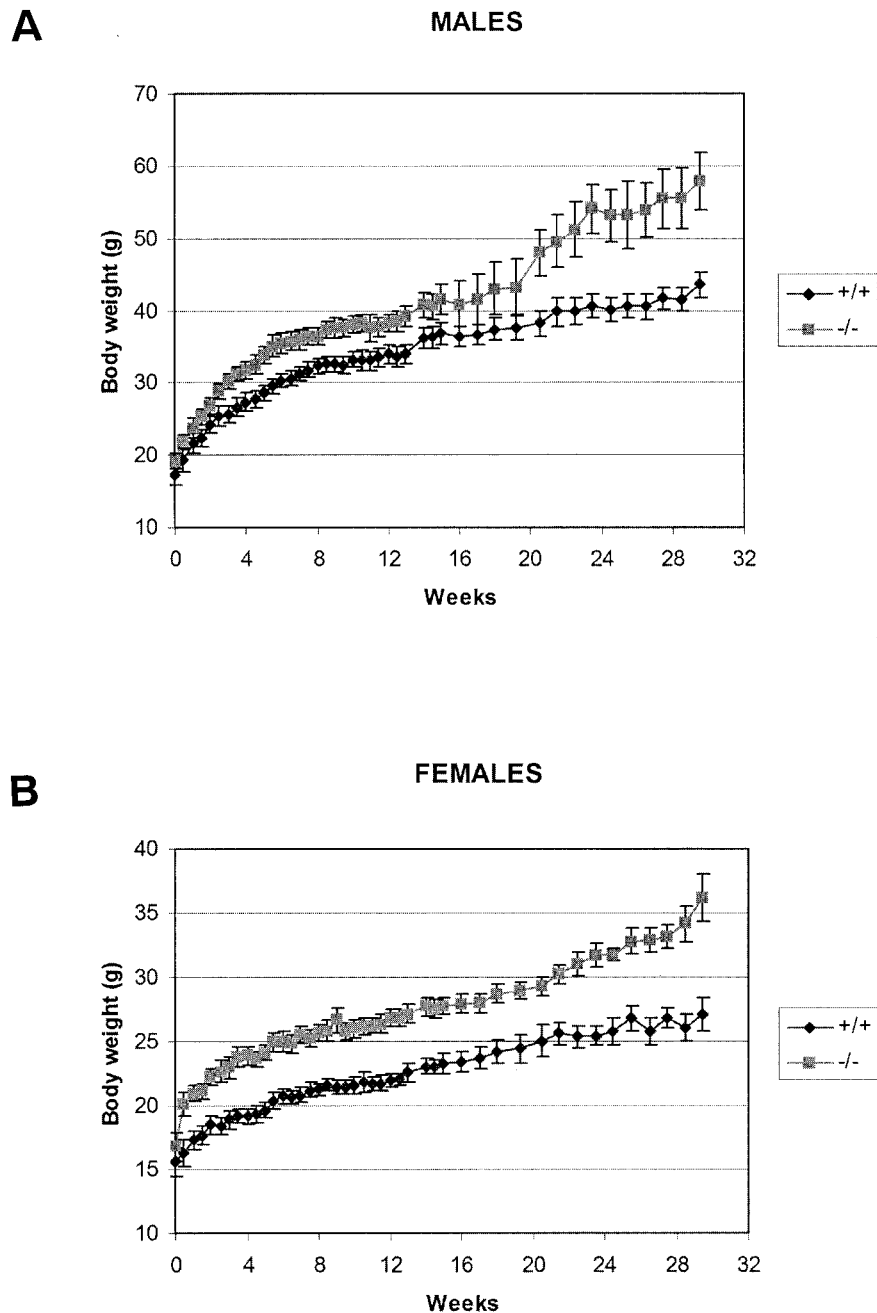


FIG. 2. Growth curve of *Mmp19*^{+/+} (◆) and *Mmp19*^{-/-} (◻) male mice (A) or female mice (B) kept on a high-fat diet.

(GenBank accession number NM.011146; forward, 5'-CCGAAGAACCATCC GATTGAAG-3', reverse, 5'-AAAAATTCGGATGGCCACCTCT-3'), *Serbp1* (GenBank accession number AF374266; forward, 5'-TTCTCTGGCCTCCTCT CTGGAA-3'; reverse, 5'-AGACCGGTAGCGTTCTCAATG-3'), *leptin* (GenBank accession number M96827; forward, 5'-AGCACTTGGTTCGCTATCGC T-3'; reverse, 5'-TTCCCACGTAGAGCGTTAGG-3'), and *Mmp2* (GenBank accession number U15209; forward, 5'-TCATACTGCCCTTCCTTCCTC-3'; reverse, 5'-CTCCAGACCTTGCCCAITTCATC-3'). Blots were rehybridized with a β -actin cDNA probe as an indicator of RNA loading.

High-fat diet treatment. Four-week-old *Mmp19*-deficient and wild-type mice (C57BL/6/129Ola mixed genetic background) were kept in microisolation cages on a 12-h day-night cycle and fed a high-fat diet containing 42% fat (Harlan TD 88137; Zeiss). Mice were weighted twice a week for the first 15 weeks and once a week for the rest of the experiment. After 30 weeks, the mice were sacrificed

by cervical dislocation. SC and GON fat pads were removed, and the wet weight was determined. Portions of the adipose tissues were immediately frozen at -80°C for RNA or protein extraction or fixed in 4% paraformaldehyde for histology. Pieces of the skin were dissected from the same region of the back and processed for histological analysis.

Zymography. Frozen SC and GON adipose tissue were incubated overnight at 4°C on a table rocker in 10 mM sodium phosphate buffer (pH 7.2) containing 150 mM NaCl, 1% Triton X-100, 0.1% sodium dodecyl sulfate (SDS), 0.5% sodium deoxycholate, and 0.2% NaN_3 . After centrifugation, the protein concentration of the supernatant was evaluated by bicinchoninic acid technique (BCA Protein Assay kit; Pierce). Then, 18 μg of nonreduced protein sample was loaded on 8% SDS-polyacrylamide gels containing 0.2% gelatin. After electrophoresis, proteins were renatured by incubating gels in 2.5% Triton X-100 for 3 h at room temperature. Gels were then washed twice in water and incubated overnight at

TABLE 1. Effect of *Mmp19*^{-/-} deficiency on adipose tissue weight and cellularity after 30 weeks of high-fat diet

Measurement	Mean \pm SEM in ^a :			
	Males		Females	
	<i>Mmp19</i> ^{+/+}	<i>Mmp19</i> ^{-/-}	<i>Mmp19</i> ^{+/+}	<i>Mmp19</i> ^{-/-}
SC fat pad (mg)	706 \pm 73	1,947 \pm 271*	274 \pm 38	866 \pm 118**
GON fat pad (mg)	1,249 \pm 156	1,912 \pm 228	80 \pm 22	491 \pm 79**
SC adipocyte surface (μm^2)	1,193 \pm 60	1,937 \pm 641	985 \pm 20	3,032 \pm 264**
GON adipocyte surface (μm^2)	2,472 \pm 199	2,202 \pm 617	1,135 \pm 81	3,040 \pm 551*
Skin adipocyte surface (μm^2)	1,350 \pm 186	1,885 \pm 545*	781 \pm 51	2,141 \pm 435*
SC adipocyte no. (cells/mm ²)	666 \pm 33	308 \pm 40**	825 \pm 50	376 \pm 58**
GON adipocyte no. (cells/mm ²)	331 \pm 39	293 \pm 25	706 \pm 39	328 \pm 19**
Skin adipocyte no. (cells/mm ²)	562 \pm 60	315 \pm 39*	842 \pm 64	487 \pm 31*

^a *, $P < 0.05$; **, $P < 0.01$ (versus the corresponding wild-type mice).

37°C in substrate buffer (20 mM Tris [pH 7.4], 5 mM CaCl₂). Gels were stained with 0.25% Coomassie blue and destained in 7.5% acetic acid.

Histological analysis. Tissues were fixed in 4% paraformaldehyde in phosphate-buffered saline and stored in 70% ethanol. Fixed tissues were embedded in paraffin by standard procedures. Blocks were sectioned (5 μm) and stained with hematoxylin and eosin. For adipose tissue evaluation, portions of GON and SC fat pads and pieces of skin were processed as described above. The SC fat pad represented the adipose tissue overlaying the posterior iliac crest and was dissected from its attachment sites to the skin. The number of adipocytes and their mean diameter were determined in 3- μm tissue sections by computer-assisted image analysis. For each sample, different sections were analyzed, and 100 adipocytes were measured. The area of the cells was calculated considering the maximum and minimum diameter of each adipocyte.

Carcinogenesis protocols and analysis of tumors. Mouse experimentation was done in accordance with the guidelines of the Universidad de Oviedo regarding the care and use of laboratory animals. For methylcholanthrene (MCA) chemical carcinogenesis, groups of *Mmp19*^{-/-} ($n = 11$) and wild-type ($n = 12$) male mice were injected SC with a freshly prepared solution of MCA in olive oil (100 μg in 100 μl per mouse) in each flank. We observed mice weekly for tumor development over the course of 22 to 30 weeks. Tumors larger than 5 mm and showing progressive growth were counted as positive and confirmed thereafter by histological analysis. Mice were killed when they had an overt tumor mass or if they looked moribund. After conventional staining with hematoxylin and eosin, cells were morphologically identified by an expert pathologist and counted with no previous knowledge of mouse genotype and time point in each slide.

Preparation of the three-dimensional aortic ring cultures. Angiogenesis was studied by culturing rings of mouse thoracic aorta in three-dimensional collagen gels as previously described (26). Briefly, 1-mm-long aortic ring-shaped fragments were embedded in a rat tail interstitial collagen gel (1.5 mg/ml) (3) prepared by mixing 7.5 volumes of 2 mg of collagen/ml (Collagen R; Serva, Heidelberg, Germany), 1 volume of 10 \times minimum essential medium (Life Technologies, Ltd., Paisley, Scotland), 1.5 volumes of NaHCO₃ (15.6 mg/ml), and 0.1 volume 1 M NaOH to adjust the pH to 7.4. The collagen gels containing the aortic rings were polymerized in cylindrical agarose wells and kept in triplicate at 37°C in 60-mm-diameter petri dishes (bacteriological polystyrene; Falcon; Becton Dickinson, Lincoln Park, N.J.). Each dish contained 6 ml of MCDB131 (Life Technologies, Ltd.) supplemented with 25 mM NaHCO₃, 2.5% mouse serum, 1% glutamine, 100 U of penicillin/ml, and 100 μg of streptomycin/ml. The cultures were kept at 37°C in a humidified environment for a week and examined every second day with an Olympus microscope at appropriate magnifications. Results were drawn from three independent assays performed in triplicate.

Quantification of angiogenesis. Image analysis was performed on a Sun SPARC30 work station with the software Visilog 5.0 from Noesis. We used an improved computer-assisted image analysis (3, 10) that allows automatic measurements of the geometrical and morphological parameters. After generation of binary image, the following automatic measurements were obtained: the number of microvessels (N_v), the maximal microvessel length (L_{max}), and the total number of branches in microvessels (N_b).

Statistical analysis. All experimental data are reported as means \pm the standard errors of the mean, and statistical analysis was performed by using the nonparametric Student t test.

RESULTS

Generation of *Mmp19*-deficient mice. To examine the in vivo function of *Mmp19*, we generated mice with a targeted mutation in the *Mmp19* gene. A genomic clone encoding *Mmp19* was obtained from a mouse 129-SV/J genomic DNA library and used for construction of the targeting vector (Fig. 1A). This vector was designed to allow the replacement of the promoter region and exons 1 and 2 of the endogenous *Mmp19* gene with a *neo* cassette (Fig. 1A). The linearized targeting vector was electroporated into HM-1 ES cells, and 10 clones that were positive for homologous recombination were used to generate chimeric founder mice. Heterozygous mice from the F₁ generation were identified by Southern blot analysis and then crossed to obtain *Mmp19*-null mice (Fig. 1B). Northern blot analysis of total RNA from diverse tissues of wild-type and knockout animals revealed that the *Mmp19* transcript was absent in homozygous null mice (Fig. 1C). The same negative results were obtained by RT-PCR of these tissues (data not shown), confirming the generation of an *Mmp19*-null allele.

Despite the *Mmp19* deficiency, these mutant mice developed normally, with males and females being fertile. Likewise, there were no gross detectable differences between the growth curves of wild-type and knockout mice. In addition, the mutant mice showed no overt phenotype, and their long-term survival rates were indistinguishable from those of their wild-type littermates. Finally, histopathologic analysis of diverse tissues in adult *Mmp19*^{-/-} animals revealed no observable differences with wild-type tissues (data not shown). Taken together, these data demonstrate that *Mmp19* is dispensable for embryonic and adult mouse development, as well as for normal growth and fertility, possibly due to functional redundancy with other members of the MMP family.

Nutritionally induced obesity in *Mmp19*-null mice. In the course of characterization of *Mmp19*-deficient mice, we noticed an increase in the body weight of aged mice that was not observed in the wild-type mice kept on standard chow. This observation prompted us to evaluate the possible role of *Mmp19* in adipose tissue biology. To this aim, wild-type and *Mmp19*-null mice were fed a high-fat diet. At the start of the study (4-week-old mice), the body weight of *Mmp19*^{-/-} mice was slightly higher (17.7 \pm 0.8 g, $n = 11$) than that of wild-type animals (16.3 \pm 0.8, $n = 16$), but this difference was not

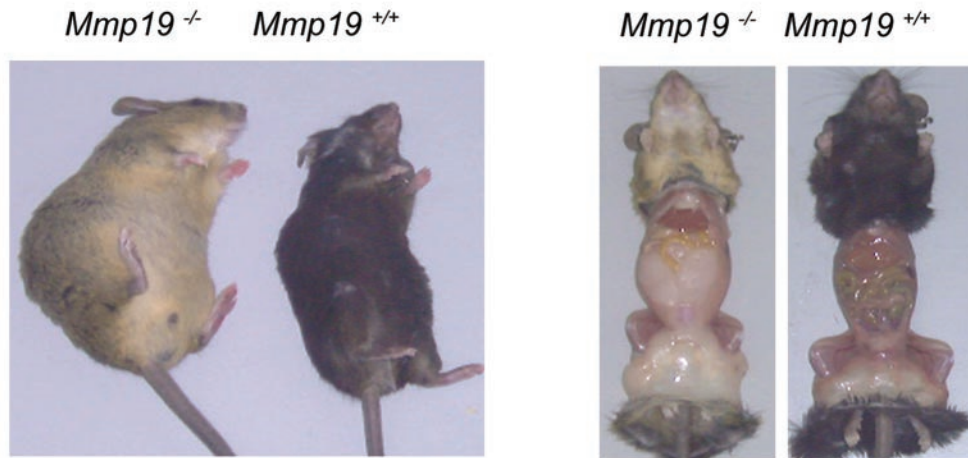
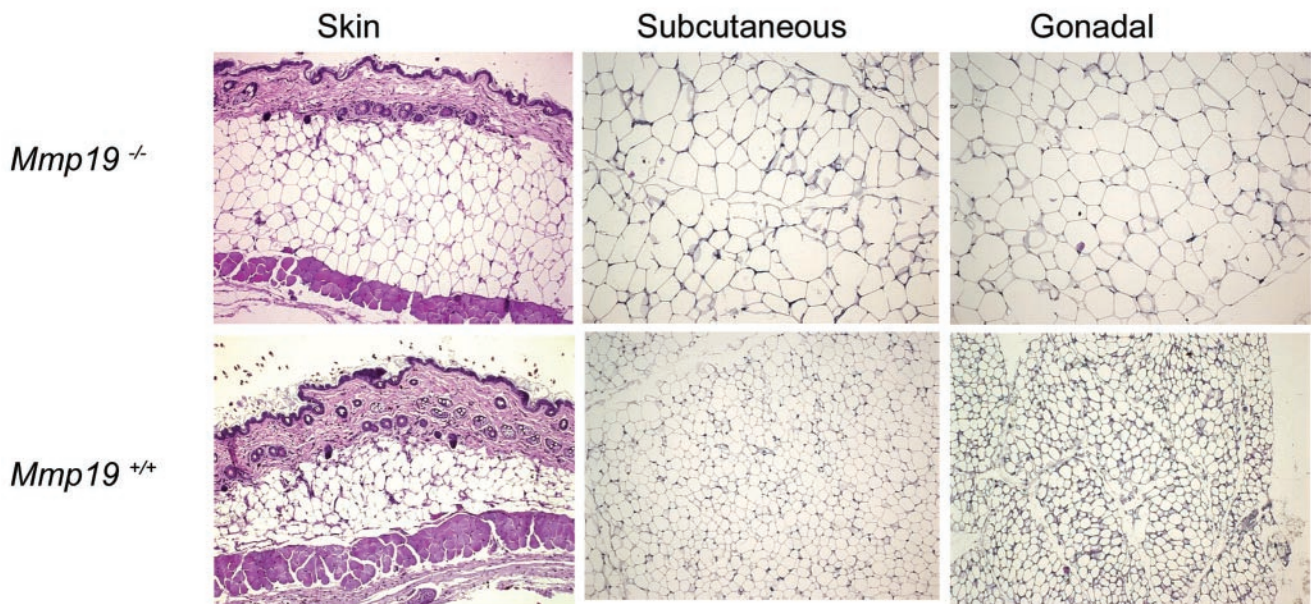
A**B**

FIG. 3. Increased body weight and adipocyte hypertrophy in *Mmp19*^{-/-} mice after 30 weeks of a high-fat diet. (A) Photographs of representative *Mmp19*^{-/-} and *Mmp19*^{+/+} mice. (B) Hematoxylin and eosin staining of skin, SC, and GON adipose tissue sections taken from *Mmp19*^{-/-} and *Mmp19*^{+/+} mice.

statistically significant. However, after 30 weeks on this high-fat diet, the body weight of the *Mmp19*^{-/-} mice was significantly higher than that of the controls (44.9 ± 4.0 g versus 34.8 ± 2.4 g; $P < 0.05$). When the growth curves were analyzed with respect to the sex of the mice (Fig. 2), there was a pronounced gain of weight in both *Mmp19*^{-/-} male and female mice compared to the corresponding groups of male and female controls (38.7 ± 4.0 versus 26.2 ± 1.6 [$P < 0.04$] and 19.6 ± 2.5 versus 11.3 ± 1.0 [$P < 0.02$]).

To determine whether the increase in body weight observed in *Mmp19*-deficient mice was due to an increase in fat content, SC and GON fat pad deposits were separately weighted. As shown in Table 1, the total weight of both fat pads was also higher in the *Mmp19*^{-/-} than in the wild-type controls, except for the GON fat deposits in the male mutants. Analysis of cellularity of the SC and GON fat pads by hematoxylin-eosin staining and morphometric measurement of adipocyte diameters revealed that the surfaces of SC, GON, and skin adipo-

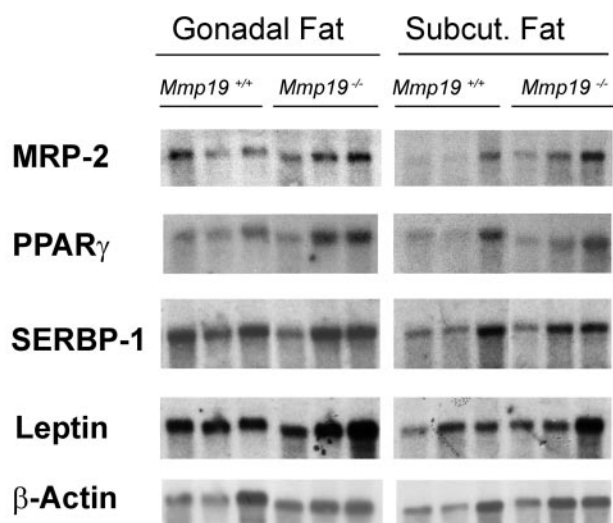


FIG. 4. Expression analysis of *Ppar γ* , *leptin*, *Srebp1*, and *Mrp2* in *Mmp19*^{-/-} and wild-type mice. RNA was prepared from GON and SC adipose tissues of three representative mice kept on a high-fat diet and analyzed by Northern blotting.

cytes from *Mmp19*-null male and female mice were bigger than those of the controls except for the GON fat pad from mutant male mice (Table 1 and Fig. 3). The number of adipocytes per surface unit was lower in *Mmp19*-deficient mice. Taken together, these results indicate that the observed diet-induced obesity in *Mmp19*-deficient mice is linked to a marked hypertrophy of the adipocytes of these mice compared to their wild-type controls. We next tried to determine whether the observed adipocyte hypertrophy in *Mmp19* mutant mice is due to an alteration of the adipocyte differentiation program. To test this possibility, we compared by Northern blot analysis the expression of key adipocyte regulators, including *Ppar γ* , *leptin*, *Srebp1*, and *Mrp2*, in GON and SC fat pads of *Mmp19*^{-/-} and wild-type mice kept on a high-fat diet. Despite the fact that these genes have been shown to be involved in various steps of adipogenesis (17, 23, 33), we were unable to detect any significant differences in their expression levels in *Mmp19*^{-/-} mice (Fig. 4).

On the other hand, it has been recently reported that *Mmp2* is the main gelatinase expressed within adipocyte tissue (25). To gain further insight into a possible differential activity of this gelatinolytic system in the absence of the *Mmp19*, we analyzed GON and SC adipose tissues from *Mmp19*^{-/-} and wild-type mice by gelatin zymography. However, similar gelatinolytic activities for pro*Mmp2* and *Mmp2* were detected in both types of mice (not shown), indicating that the absence of *Mmp19* is not compensated for by an increase in the activity of the major adipocyte gelatinase.

***Mmp19*-deficient mice are more resistant to the development of MCA-induced fibrosarcomas.** MMP-19 has been detected in dermal fibroblasts and keratinocytes of human skin, as well as in inflammatory cells such as monocytes and macrophages, suggesting a role for this protease in inflammatory processes and skin tumorigenesis (14, 35). To evaluate this possibility, wild-type and *Mmp19* mutant male mice were subjected to a skin carcinogenesis protocol based on the intrader-

mal injection of a single dose of the chemical carcinogen MCA. As shown in Fig. 5A, fibrosarcomas arose more rapidly and with a significantly higher incidence in wild-type mice than in *Mmp19*-deficient mice. These differences in the number of fibrosarcomas between mutant mice and wild-type controls were statistically significant ($P < 0.05$). Histological analysis of the fibrosarcomas generated in both wild-type and *Mmp19*^{-/-} male mice revealed that most of them (80%) were undifferentiated and invasive grade III fibrosarcomas (Fig. 5B), suggesting that the absence of *Mmp19* does not influence the late stages of tumor development in male mice. In addition, Northern blot analysis of MCA-induced fibrosarcomas in wild-type mice revealed a high level of expression of *Mmp19* in these malignant tumors (data not shown), reflecting its putative relevance in the carcinogenesis process.

To evaluate the possibility that reduced tumor susceptibility in mutant mice could be due to angiogenesis deficiencies derived from the absence of this protease, we compared this process in knockout and wild-type animals by using a quantitative angiogenesis model. Segments of mouse thoracic aortas embedded in a collagen gel were cultured in MCDB131 medium containing autologous serum (2.5% final concentration). During the first 4 days of culture, isolated fibroblast-like cells migrated into the gel. Subsequently, microvessel outgrowths arose from the edges of the parental vessel where the basement membrane had been ruptured. As shown in Fig. 6, no differences were observed in the number of microvessels (N_v , 7 ± 4 versus 7 ± 5), the number of branchings (N_b , 14.5 ± 7 versus 15 ± 7), and the length of the vessels (L_{max} , 1.12 ± 0.4 mm versus 1.04 ± 0.32 mm) between mutant and wild-type mice, respectively. The angiogenic response in the mice aortic ring assay was not dependent on the presence or absence of *Mmp19*, indicating that this protease does not play a critical role in angiogenesis in this experimental model.

DISCUSSION

We describe here the generation and phenotype analysis of mutant mice deficient in *Mmp19*, a member of the MMP family of endopeptidases with a wide tissue-distribution and a series of structural and enzymatic characteristics that do not allow its classification in any of the well-established MMP subfamilies, including collagenases, stromelysins, gelatinases, and membrane-type MMPs. However, and despite the wide expression pattern of *Mmp19* under normal quiescent conditions, targeted disruption of this gene in mice does not cause any major abnormalities. Thus, and similar to most cases of mice deficient in single specific MMPs, *Mmp19*-null mice develop normally, are fertile, and have long-term survival rates indistinguishable from those of wild-type mice. Nevertheless, further analysis of *Mmp19*^{-/-} mice subjected to diverse challenges has allowed us to uncover the involvement of this enzyme in different normal and pathological processes. Our first studies in this regard were derived from the observation that aged mutant mice exhibited an increase in body weight compared to control littermates. These differences were significantly enhanced when mice were fed a high-fat diet, suggesting that *Mmp19* could be somewhat involved in regulating adipogenesis, as reported for other proteases of different catalytic classes (15, 16, 20, 29, 37). Histopathologic analysis revealed

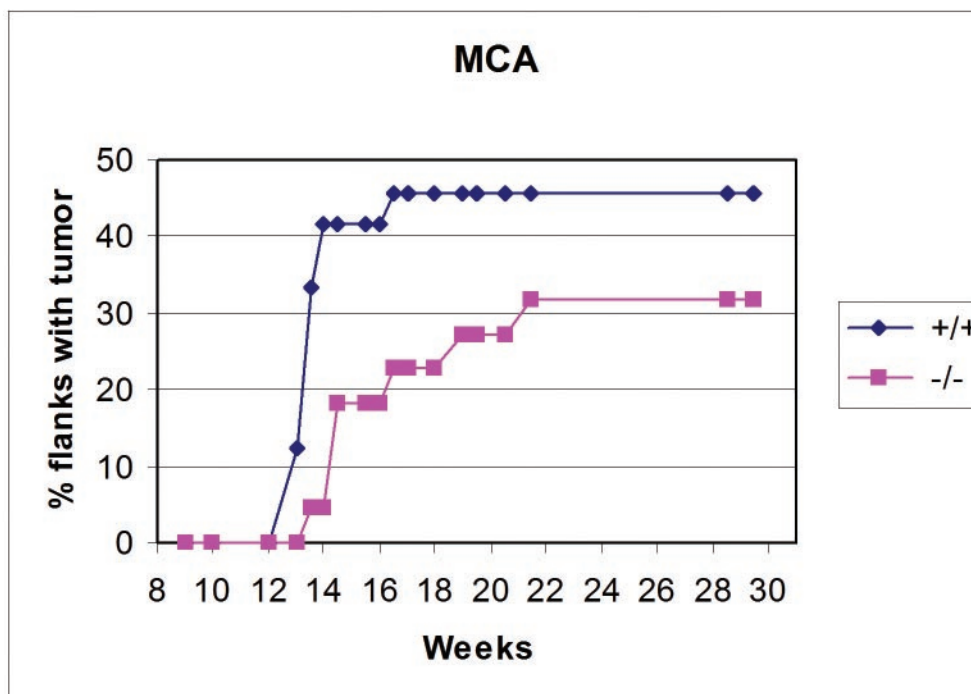
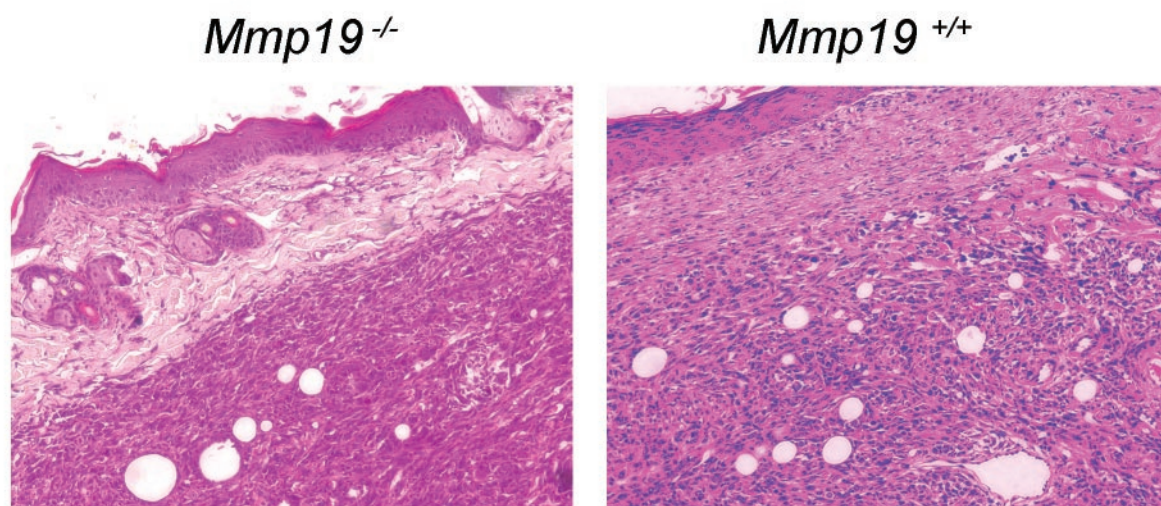
A**B**

FIG. 5. Skin tumorigenesis in *Mmp19^{-/-}* and wild-type mice. (A) Percentage of flanks with tumor of *Mmp19^{+/+}* (◆) or *Mmp19^{-/-}* (■) male mice injected with 100 μ g of MCA; (B) histopathologic analysis of skin tumors generated in wild-type and *Mmp19^{-/-}* male mice.

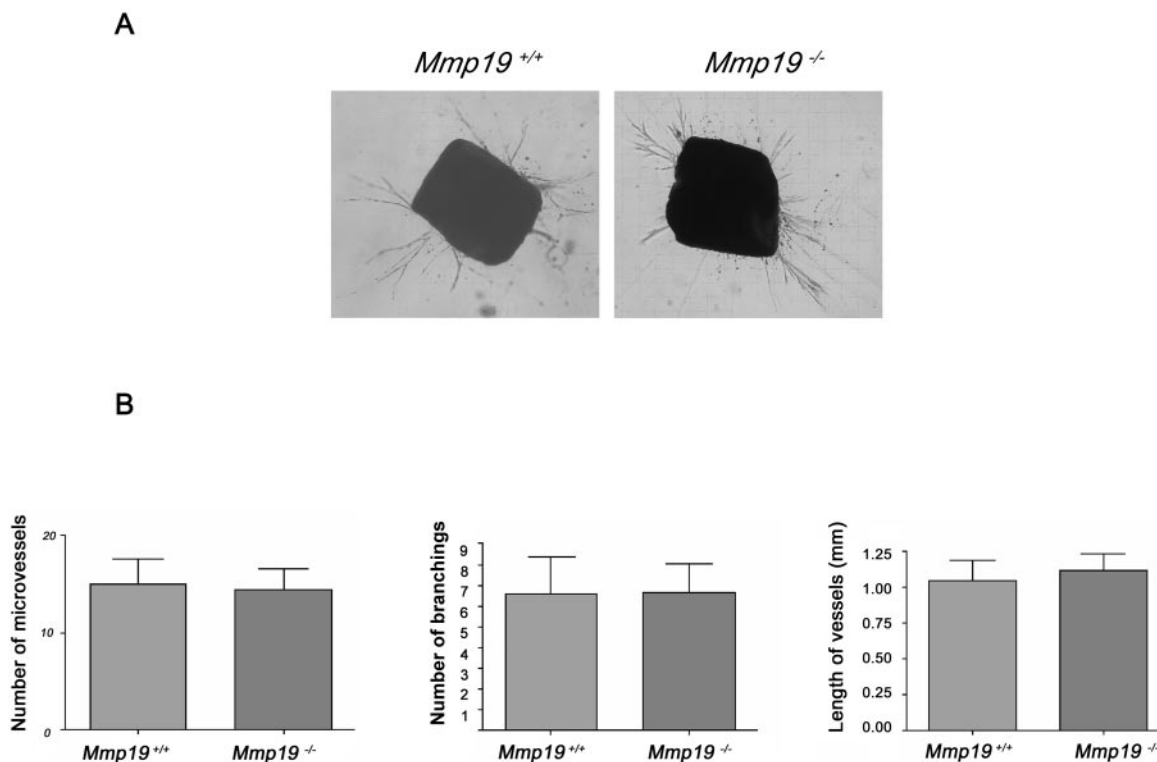


FIG. 6. Capillary outgrowth from mouse aortic rings of *Mmp19*^{-/-} and wild-type mice. (A) Segments of mouse thoracic aortas from *Mmp19*^{+/+} and *Mmp19*^{-/-} mice; (B) quantification in the aortic ring assay of the number of microvessels, the number of branchings, and the length of the vessels of *Mmp19*^{-/-} and wild-type mice.

that the increased body weight observed in *Mmp19*-null mice is due to an overall increase in both SC and GON fat pad deposits, which in turn is caused by a marked adipocyte hypertrophy in these mice compared to their wild-type controls. Taken together, these findings indicate that *Mmp19* is a negative regulator of adipose tissue formation.

The role of MMPs in adipose tissue remodeling has been demonstrated in several studies, but most of these studies have concluded that MMPs are positive regulators of this process (4, 6, 9, 21, 25). Thus, several studies have independently shown that treatment of preadipocyte cell lines with synthetic MMP inhibitors blocks the adipocyte differentiation process (4, 9, 25). Likewise, treatment with MMP inhibitors impairs adipose tissue development in mice fed a high-fat diet (21). Furthermore, the secretion of MMP-2 and MMP-9 increases during adipocyte differentiation in both human adipocytes and mouse preadipocyte cell lines, suggesting that these Mmps contribute to adipogenesis by promoting adipocyte differentiation (4, 6, 25). However, there are at least two additional MMPs that appear to play inhibitory roles in adipogenesis that are similar to those here reported for *Mmp19*. Mice deficient for *Mmp3* show accelerated adipogenesis during mammary gland involution and enhanced diet-induced adipose tissue development (1, 24), whereas *Mmp11*-null mice display a nutritionally induced obesity whose molecular basis has not been reported yet (22). Likewise, at present we can only speculate about the potential role of *Mmp19* as a negative regulator of adipogenesis. Thus, the wide substrate specificity of *Mmp19* could facilitate the degradation of different extracellular matrix components that

could provide inhibitory signals to adipocytes. The recent finding that *Mmp19* is also upregulated in obese adipose tissue and during differentiation of 3T3-L1 preadipocytes into adipocytes (6, 25) could be indicative of the coexistence of opposing growth and differentiation signals triggered by Mmps. Some family members such as *Mmp2* and *Mmp9* could remodel the extracellular matrix of adipogenic cells to facilitate the adipogenic process, whereas *Mmp19* and other related enzymes could function in an opposite manner, slowing down or blocking this process. Alternatively, *Mmp19* could regulate the bioavailability of adipocyte growth factors sequestered as inactive molecules in the matrix or blocked by interaction with their binding proteins. The recent finding that *Mmp19* cleaves *in vitro* IGFBP3 (34) suggests that this protease could control the activity of insulin-like growth factors in adipose tissue and contribute to the modulation of adipocyte growth. Nevertheless, we did not observe variations in the molecular forms of the different components of the IGFBP system when we compared mutant and wild-type liver extracts by means of a Western ligand blot (data not shown), suggesting that these factors are not major *in vivo* substrates for this enzyme. Further studies now in progress will be required to identify the specific substrates mediating the observed inhibitory function of *Mmp19* during adipogenesis.

The dispensability of *Mmp19* during adult mouse development has also facilitated the analysis of cancer susceptibility in *Mmp19*-null mice, an aspect of growing interest after the finding of dual and important roles of these enzymes in tumor progression (2, 8, 11, 12, 30). Our studies with *Mmp19*^{-/-} mice

have shown that, after a typical MCA-induced chemical carcinogenesis protocol, these mutant mice develop fewer fibrosarcomas and with a longer latency period than wild-type littermates. Therefore, and similar to the situation previously described for most MMP family members, these *in vivo* experiments indicate that *Mmp19* facilitates tumor progression. The role of *Mmp19* in promoting cancer progression could be due to their ability to degrade a variety of extracellular matrix and basement membrane components, such as type IV collagen, fibronectin, tenascin-C, laminin, or nidogen, thereby facilitating the generation of a microenvironment permissive for tumor cell growth. However, recent studies have shown that the role of MMPs in cancer progression is much more complex than that derived from their direct degradative action on extracellular matrix components (11, 12). These additional functions mediated by MMPs include activation of growth factors, suppression of tumor cell apoptosis, release of angiogenic factors, or destruction of chemokine gradients generated by the host immune response. Accordingly, proteolytic processing of some of these bioactive molecules by *Mmp19* could also contribute to the formation of the stromal environment necessary to promote malignant transformation and/or tumor growth in early stages of cancer. Because *Mmp19* has been previously reported to be produced by endothelial cells and to possess angiogenic properties (18), we evaluated the hypothesis that the *Mmp19* role in tumor progression could be linked to its proangiogenic functions. However, the *ex vivo* angiogenic potential of microvessels from aortic rings was not affected by *Mmp19* deficiency, indicating that this process does not appear to be an important factor in the altered cancer susceptibility caused by the loss of this protease in *Mmp19*^{-/-} mice. Therefore, and similar to the case of the nutritionally induced obesity observed in *Mmp19*-null mice, further studies will be required to identify the mechanisms underlying the stimulatory action of *Mmp19* in tumor progression.

In summary, the generation of mutant mice deficient in *Mmp19* has identified new *in vivo* roles for this proteolytic enzyme and provided a new model to study the relevance of protease-mediated processes taking place in adipogenesis or during tumor progression. Hopefully, these studies could contribute to the development of better therapeutic strategies for two major and growing medical problems: obesity and cancer.

ACKNOWLEDGMENTS

We thank Marta S. Pitiot, Aitana Vallina, and Joanne Shi for excellent technical assistance; A. Fueyo for advice in carcinogenesis assays; D. Melton for the generous gift of the HM-1 ES cells; and the NIDCR Gene Targeting Facility for assistance with the generation of knockout mice.

This study was supported by grants from Comisión Interministerial de Ciencia y Tecnología (SAF03-0258), the European Union (FP5 and FP6), HHS/NIH/NIDCR of the U.S. Government, and Gobierno del Principado de Asturias. The Instituto Universitario de Oncología is supported by RTICCC and Obra Social Cajastur-Asturias of Spain.

REFERENCES

- Alexander, C. M., S. Selvarajan, J. Mudgett, and Z. Werb. 2001. Stromelysin-1 regulates adipogenesis during mammary gland involution. *J. Cell Biol.* **152**:693–703.
- Balbin, M., A. Fueyo, A. M. Tester, A. M. Pendas, A. S. Pitiot, A. Astudillo, C. M. Overall, S. D. Shapiro, and C. Lopez-Otin. 2003. Loss of collagenase-2 confers increased skin tumor susceptibility to male mice. *Nat. Genet.* **35**:252–257.
- Blacher, S., L. Devy, M. F. Burbridge, G. Roland, G. Tucker, A. Noel, and J. M. Foidart. 2001. Improved quantification of angiogenesis in the rat aortic ring assay. *Angiogenesis* **4**:133–142.
- Bouloumie, A., C. Sengenès, G. Portolan, J. Galitzky, and M. Lafontan. 2001. Adipocyte produces matrix metalloproteinases 2 and 9: involvement in adipose differentiation. *Diabetes* **50**:2080–2086.
- Brinckerhoff, C. E., and L. M. Matrisian. 2002. Matrix metalloproteinases: a tail of a frog that became a prince. *Nat. Rev. Mol. Cell. Biol.* **3**:207–214.
- Chavey, C., B. Mari, M. N. Monthouel, S. Bonnafous, P. Anglard, E. Van Obberghen, and S. Tartare-Deckert. 2003. Matrix metalloproteinases are differentially expressed in adipose tissue during obesity and modulate adipocyte differentiation. *J. Biol. Chem.* **278**:11888–11896.
- Cossins, J., T. J. Dudgeon, G. Catlin, A. J. Gearing, and J. M. Clements. 1996. Identification of MMP-18, a putative novel human matrix metalloproteinase. *Biochem. Biophys. Res. Commun.* **228**:494–498.
- Coussens, L. M., B. Fingleton, and L. M. Matrisian. 2002. Matrix metalloproteinase inhibitors and cancer: trials and tribulations. *Science* **295**:2387–2392.
- Croissandeau, G., M. Chretien, and M. Mbikay. 2002. Involvement of matrix metalloproteinases in the adipose conversion of 3T3-L1 preadipocytes. *Biochem. J.* **364**:739–746.
- Devy, L., S. Blacher, C. Grignet-Debrus, K. Bajou, V. Masson, R. D. Gerard, A. Gils, G. Carmeliet, P. Carmeliet, P. J. Declercq, A. Noel, and J. M. Foidart. 2002. The pro- or antiangiogenic effect of plasminogen activator inhibitor 1 is dose dependent. *FASEB J.* **16**:147–154.
- Egeblad, M., and Z. Werb. 2002. New functions for the matrix metalloproteinases in cancer progression. *Nat. Rev. Cancer.* **2**:161–174.
- Freije, J. M., M. Balbin, A. M. Pendas, L. M. Sanchez, X. S. Puente, and C. Lopez-Otin. 2003. Matrix metalloproteinases and tumor progression. *Adv. Exp. Med. Biol.* **532**:91–107.
- Halpert, I., U. I. Sires, J. D. Roby, S. Potter-Perigo, T. N. Wight, S. D. Shapiro, H. G. Welgus, S. A. Wickline, and W. C. Parks. 1996. Matrilysin is expressed by lipid-laden macrophages at sites of potential rupture in atherosclerotic lesions and localizes to areas of versican deposition, a proteoglycan substrate for the enzyme. *Proc. Natl. Acad. Sci. USA* **93**:9748–9753.
- Hietala, N., U. Impola, C. Lopez-Otin, U. Saarialho-Kere, and V. M. Kahari. 2003. Matrix metalloproteinase-19 expression in dermal wounds and by fibroblasts in culture. *J. Invest. Dermatol.* **121**:997–1004.
- Jackson, R. S., J. W. Creemers, S. Ohagi, M. L. Raffin-Sanson, L. Sanders, C. T. Montague, J. C. Hutton, and S. O'Rahilly. 1997. Obesity and impaired prohormone processing associated with mutations in the human prohormone convertase 1 gene. *Nat. Genet.* **16**:303–306.
- Kawaguchi, N., X. Xu, R. Tajima, P. Kronqvist, C. Sundberg, F. Loechel, R. Albrechtsen, and U. M. Wewer. 2002. ADAM 12 protease induces adipogenesis in transgenic mice. *Am. J. Pathol.* **160**:1895–1903.
- Kim, C. S., T. Kawada, H. Yoo, B. S. Kwon, and R. Yu. 2003. Macrophage inflammatory protein-related protein-2, a novel CC chemokine, can regulate preadipocyte migration and adipocyte differentiation. *FEBS Lett.* **548**:125–130.
- Kolb, C., S. Mauch, U. Krawinkel, and R. Sedlacek. 1999. Matrix metalloproteinase-19 in capillary endothelial cells: expression in acutely, but not in chronically, inflamed synovium. *Exp. Cell Res.* **250**:122–130.
- Kontinen, Y. T., M. Ainola, H. Valleala, J. Ma, H. Ida, J. Mandelin, R. W. Kinne, S. Santavirta, T. Sorsa, C. Lopez-Otin, and M. Takagi. 1999. Analysis of 16 different matrix metalloproteinases (MMP-1 to MMP-20) in the synovial membrane: different profiles in trauma and rheumatoid arthritis. *Ann. Rheum. Dis.* **58**:691–697.
- Kurisaki, T., A. Masuda, K. Sudo, J. Sakagami, S. Higashiyama, Y. Matsuda, A. Nagabukuro, A. Tsuji, Y. Nabeshima, M. Asano, Y. Iwakura, and A. Sehara-Fujisawa. 2003. Phenotypic analysis of Meltrin alpha (ADAM12)-deficient mice: involvement of Meltrin alpha in adipogenesis and myogenesis. *Mol. Cell. Biol.* **23**:55–61.
- Lijnen, H. R., E. Maquoi, L. B. Hansen, B. Van Hoef, L. Frederix, and D. Collen. 2002. Matrix metalloproteinase inhibition impairs adipose tissue development in mice. *Arterioscler. Thromb. Vasc. Biol.* **22**:374–379.
- Lijnen, H. R., H. B. Van, L. Frederix, M. C. Rio, and D. Collen. 2002. Adipocyte hypertrophy in stromelysin-3 deficient mice with nutritionally induced obesity. *Thromb. Haemost.* **87**:530–535.
- MacDougald, O. A., and S. Mandrup. 2002. Adipogenesis: forces that tip the scales. *Trends Endocrinol. Metab.* **13**:5–11.
- Maquoi, E., D. Demeulemeester, G. Voros, D. Collen, and H. R. Lijnen. 2003. Enhanced nutritionally induced adipose tissue development in mice with stromelysin-1 gene inactivation. *Thromb. Haemost.* **89**:696–704.
- Maquoi, E., C. Munaut, A. Colige, D. Collen, and H. R. Lijnen. 2002. Modulation of adipose tissue expression of murine matrix metalloproteinases and their tissue inhibitors with obesity. *Diabetes* **51**:1093–1101.
- Masson, V. V., L. Devy, C. Grignet-Debrus, S. Bernt, K. Bajou, S. Blacher, G. Roland, Y. Chang, T. Fong, P. Carmeliet, J. M. Foidart, and A. Noel. 2002. Mouse aortic ring assay: a new approach of the molecular genetics of angiogenesis. *Biol. Proced. Online* **4**:24–31.
- Mueller, M. S., S. Mauch, and R. Sedlacek. 2000. Structure of the human MMP-19 gene. *Gene* **252**:27–37.

28. Nagase, H., and J. F. Woessner, Jr. 1999. Matrix metalloproteinases. *J. Biol. Chem.* **274**:21491–21494.
29. Naggert, J. K., L. D. Fricker, O. Varlamov, P. M. Nishina, Y. Rouille, D. F. Steiner, R. J. Carroll, B. J. Paigen, and E. H. Leiter. 1995. Hyperproinsulinemia in obese fat/fat mice associated with a carboxypeptidase E mutation which reduces enzyme activity. *Nat. Genet.* **10**:135–142.
30. Overall, C. M., and C. Lopez-Otin. 2002. Strategies for MMP inhibition in cancer: innovations for the post-trial era. *Nat. Rev. Cancer.* **2**:657–672.
31. Pendas, A. M., M. Balbin, E. Llano, M. G. Jimenez, and C. Lopez-Otin. 1997. Structural analysis and promoter characterization of the human collagenase-3 gene (MMP13). *Genomics* **40**:222–233.
32. Pendas, A. M., V. Knauper, X. S. Puente, E. Llano, M. G. Mattei, S. Apte, G. Murphy, and C. Lopez-Otin. 1997. Identification and characterization of a novel human matrix metalloproteinase with unique structural characteristics, chromosomal location, and tissue distribution. *J. Biol. Chem.* **272**:4281–4286.
33. Rangwala, S. M., and M. A. Lazar. 2000. Transcriptional control of adipogenesis. *Annu. Rev. Nutr.* **20**:535–559.
34. Sadowski, T., S. Dietrich, F. Koschinsky, and R. Sedlacek. 2003. Matrix metalloproteinase 19 regulates insulin-like growth factor-mediated proliferation, migration, and adhesion in human keratinocytes through proteolysis of insulin-like growth factor binding protein-3. *Mol. Biol. Cell* **14**:4569–4580.
35. Sadowski, T., S. Dietrich, M. Muller, B. Havlickova, M. Schunck, E. Proksch, M. S. Muller, and R. Sedlacek. 2003. Matrix metalloproteinase-19 expression in normal and diseased skin: dysregulation by epidermal proliferation. *J. Invest. Dermatol.* **121**:989–996.
36. Sedlacek, R., S. Mauch, B. Kolb, C. Schatzlein, H. Eibel, H. H. Peter, J. Schmitt, and U. Krawinkel. 1998. Matrix metalloproteinase MMP-19 (RASI-1) is expressed on the surface of activated peripheral blood mononuclear cells and is detected as an autoantigen in rheumatoid arthritis. *Immunobiology* **198**:408–423.
37. Selvarajan, S., L. R. Lund, T. Takeuchi, C. S. Craik, and Z. Werb. 2001. A plasma kallikrein-dependent plasminogen cascade required for adipocyte differentiation. *Nat. Cell Biol.* **3**:267–275.
38. Stracke, J. O., A. J. Fosang, K. Last, F. A. Mercuri, A. M. Pendas, E. Llano, R. Perris, P. E. Di Cesare, G. Murphy, and V. Knauper. 2000. Matrix metalloproteinases 19 and 20 cleave aggrecan and cartilage oligomeric matrix protein (COMP). *FEBS Lett.* **478**:52–56.
39. Stracke, J. O., M. Hutton, M. Stewart, A. M. Pendas, B. Smith, C. Lopez-Otin, G. Murphy, and V. Knauper. 2000. Biochemical characterization of the catalytic domain of human matrix metalloproteinase 19: evidence for a role as a potent basement membrane degrading enzyme. *J. Biol. Chem.* **275**:14809–14816.
40. Vu, T. H., and Z. Werb. 2000. Matrix metalloproteinases: effectors of development and normal physiology. *Genes Dev.* **14**:2123–2133.
41. Yang, M., and M. Kurkinen. 1998. Cloning and characterization of a novel matrix metalloproteinase (MMP), CMMP, from chicken embryo fibroblasts. CMMP, *Xenopus* XMMP, and human MMP19 have a conserved unique cysteine in the catalytic domain. *J. Biol. Chem.* **273**:17893–17900.